Advances in Nano Research, *Vol. 10, No. 5 (2021) 493-507*
DOI: https://doi.org/10.12989/anr.2021.10.5.493

Buckling of porosity-dependent bi-directional FG nanotube using numerical method

Haiquan Wang*[1], Yousef Zandi[2], Morteza Gholizadeh[2] and Alibek Issakhov[3,4]

[1]*Chemistry and Chemical Engineering & Environmental College, Weifang University, Weifang 261061, Shandong, China*
[2]*Department of Civil Engineering, Tabriz Branch, Islamic Azad University, Tabriz, Iran*
[3]*Al-Farabi Kazakh National University, Almaty, Kazakhstan*
[4]*Kazakh-British Technical University, Almaty, Kazakhstan*

(*Received January 30, 2021, Revised April 13, 2021, Accepted April 21, 2021*)

Abstract. This article focused on studying the buckling behavior of two-dimensional functionally graded (2D-FG) nanosize tubes, including porosity based on first shear deformation and higher-order theory of tube. The nano-scale tube is simulated based on the nonlocal gradient strain theory, and the general equations and boundary conditions are derived using Hamilton's principle for the Zhang-Fu's tube model (as higher-order theory) and Timoshenko beam theory. Finally, the derived equations are solved using a numerical method for both simply-supported and clamped boundary conditions. The parametric study is performed to study the effects of different parameters such as axial and radial FG power indexes, porosity parameter, nonlocal gradient strain parameters on the buckling behavior of di-dimensional functionally graded porous tube.

Keywords: nonlocal strain gradient theory; buckling; Zhang-Fu's tube model; Timoshenko theory; two-dimensional functionally graded materials; nanotubes; higher-order theory

1. Introduction

Functionally graded materials (FGMs) are certified to have vast applications such as biomedical purposes, Dental implants, Sensors, Thermo-generators, and wear-resistant coatings. FGMs possess many advantages, including decreasing in-plane and transverse through-the-thickness stresses, enhanced thermal strength, improved residual stress distribution, higher fracture toughness, reduced stress intensity factors, and high wear resistance. Therefore, accurate ascertainment of the deformations and other behaviors of such structures is essential.

Classical theories are incomplete in modeling the small-scale effect in nano or micro size. To accurate mathematical modeling in the small-scale such as the nanotubes, some theories have emerged. One of these theories is Eringen's nonlocal theory, which considers the stress at a reference point a function of the strain at the reference point and the strains at all other points in the whole body (Eringen 1983). Also, the strain gradient theory assumes that the materials must be considered atoms with the higher-order deformation mechanism at the micro/nanoscale rather than just modeling them as collections of points. The nonlocal strain gradient theory considers nonlocal elastic stress and strain gradient stress fields using two-scale parameters (Ma *et al*. 2018). The nonlocal strain gradient theory (NSGT) proposed by Lim *et al*. (2015) results from the combination of the nonlocal stress theory of Eringen (1983) and the strain gradient theory of Aifantis (1992) and Mindlin (1965).

According to the vast application of FGMs, a structure that FGMs have made has been noticed by researchers, and the FG nanotubes are one of the most famous structures that have been focused on Azimi *et al*. (2016), Ghadiri *et al*. (2016, 2017a, b, c), Habibi *et al*. (2016), Shafiei *et al*. (2016a, b, 2019), Ebrahimi *et al*. (2017), Mirjavadi *et al*. (2017a, b, c), Shafiei and Kazemi (2017), Shafiei (2017), Shivanian *et al*. (2017), Esmailpoor *et al*. (2019), Ghabussi *et al*. (2019), Al-Furjan *et al*. (2020a, b), Alipour *et al*. (2020), Ghabussi *et al*. (2020), Jermsittiparsert *et al*. (2020), Huang *et al*. (2021). Nanotube was introduced by Kar *et al*. (1813) and there are many applications introduced for these structures such as sensors diodes, solar cells, etc. Because of their wide range applications, these nanostructures are being studied from different aspects such as vibration (Ehyaei *et al*. 2017, Akbas 2018, Aydogdu *et al*. 2018, Wu *et al*. 2018, Bendaho *et al*. 2019, Berghouti *et al*. 2019, Hussain *et al*. 2019, Uzun and Civalek 2019, Matouk *et al*. 2020, Noroozi *et al*. 2020), deflection (Eltaher *et al*. 2016, Ebrahimi and Barati 2019), electrocatalytic (Luo *et al*. 2001, Bravo *et al*. 2015), etc.

Besides many different aspects of nanotube and nanobeam behaviors, buckling behavior is one of the most significant nanotube issues considered by the researchers during the past decades (Tounsi *et al*. 2013, Besseghier *et al*. 2015, Chemi *et al*. 2015, Eltaher *et al*. 2016, 2019, Elmerabet *et al*. 2017, Bensattalah *et al*. 2018, Mehar and Panda 2019, Semmah *et al*. 2019, Nejadi and Mohammadimehr 2020).

Buckling analysis of functionally graded nanotubes are

*Corresponding author, Ph.D.,
E-mail: haiquan202@hotmail.com

ISSN: 2287-237X (Print), 2287-2388 (Online)

the main focus of many studies among the researchers. Lei *et al*. (2013) studied the buckling behavior of functionally graded carbon nanotube-reinforced composite (FG-CNTRC) plates. Jam and Kiani (2015) investigated the buckling of nanocomposite conical shells reinforced with carbon nanotubes. Wu *et al*. (2015) studied the vibration and elastic buckling of sandwich beams with a stiff core and functionally graded carbon nanotube reinforced composite (FG-CNTRC) face sheets. Moradi-Dastjerdi and Malek-Mohammadi (2017) studied the biaxial buckling of FG nanosandwich plates reinforced by carbon nanotube. Shams and Soltani (2017) studied the buckling behavior of FG carbon nanotube-reinforced plates. García-Macías *et al*. (2017) studied the compressive load effects on the buckling analysis of functionally graded carbon-nanotube reinforced cylindrical curved panels. Wang *et al*. (2021) studied the nano-scale tube reinforced FG plate's buckling analysis based on the first shear deformation theory using the numerical meshless method. Arshid *et al*. (2021) investigated the imperfect FG micro-dimension tube based on the higher-order beam theory and modified couple stress theory in the thermal environment. Foroutan *et al*. (2021) indicated the buckling behavior of carbon nano-dimension tubes made of FG material in the radius direction with the nonlinear temperature distribution and the viscous foundation based on the classic shell theory using a numerical method. Mohamed *et al*. (2020) studied the post-buckling behavior of nanosize tube rested in the elastic foundation using the Euler-Bernoulli theory of beam and DQM. Malikan *et al*. (2020) focused on the double-walled nano-scale tube's buckling using the nonlocal approach to study the effect of some parameters on it. Malikan (2020) studied the nano-dimension tube's buckling to indicated the plastic behavior based on the classic beam theory, NGT using the semi-analytical method. Malikan and Eremeyev (2020) studied the post-buckling of tapered nano-scale tubes rested in a nonlinear foundation. They worked on different boundary conditions, including surface effect, and the equation is solved by the Rayleigh method. The molecular mechanics is used to study the post-buckling and buckling of nanosize carbon tube by Genoese *et al*. (2020). On the other hand, Goel *et al*. (2020) studied the failure mechanic test of the nanosize tube using the molecular dynamic (MD) method, and they showed how the topological defect effect on buckling of tubes. Moreover, the torsional buckling of nanosize tube by MD was shown by Wallace, Chen *et al*. (2020). Also, Zeighampour and Tadi Beni (2020) indicated the behavior of buckling of boron-nitride based on different vacancy defect by MD. Bian and Wang (2020) investigated the influence of temperature on the double-tube buckling based on the nonlocal theory to model the nano-dimension and Timoshenko for deriving the equations. Amiri *et al*. (2020) studied static analysis of thick tube of carbon, based the higher-order theory of beam and using modified couple stress theory, and energy method rested in an elastic foundation in the thermal environment. Zghal *et al*. (2020) studied the analysis of post-buckling of the plate made by carbon nanotube under various mechanical loading. Li *et al*. (2020) used the shell theory to study the buckling behavior of nanotubes. Bensattalah *et al*. (2020) studied the nonlocal buckling of triple-walled tubes, including the van-der-Waals interaction.

Based on the mentioned literature review on the mechanical and thermal buckling of FG nano-scale tubes, there are many studies on the discussed topic, however, the research on the buckling analysis of bi-directional and imperfect functionally graded nano-scale tubes needs more consideration. Hence, in this article, the mechanical buckling behavior of two-dimensional functionally graded (2D-FG) nanotube, including the porosity, was investigated based on the Timoshenko beam theory and higher-order tube theory. The nonlocal gradient strain theory is used to determine the size effect of the nano-scale tube. The linear equations of motion related to nonlocal boundary conditions are derived based on the Hamilton principle and have solved by GDQM. The presented results show the effect of different parameters, such as the FG indexes, porosity parameter, small-scale parameter, etc., on the static behavior of nanotubes and can help develop and design nano-electro-mechanical systems (NEMS), nanosensors, and nano actuators.

2. Theory and formulation

2.1 Tubes structures

The material of the analyzed nanotubes is 2D-FG made of metal and ceramic which have variable material volume fraction along x and r directions. A nanotube of length (L), inner radius (Ri) and initial outer radius (Ro) is considered as shown in Fig. 1.

A cylindrical coordinate system O (x, r, θ) is defined with x in the length direction, r in the radial direction and θ in the circumferential direction. Meanwhile, the nanotube is also referred to by a rectangular coordinate system O (x, y, z), the corresponding displacement components are denoted by u_1, u_2, and u_3, respectively, and

$$y = r\cos(\theta), \qquad z = r\sin(\theta), \qquad r^2 = y^2 + z^2 \quad (1)$$

The variation of the material composition along the radius (n) is shown in Fig. 1. So, the mechanical properties of the nanotubes such as Young's modulus (E), Poisson's ratio (ν), shear modulus (G) and mass density (ρ) vary along the radius directions (r-axis).

$$F(r) = F_m + (F_c - F_m)\left(\frac{r - Ri}{Ro - Ri}\right)^{n_R}\left(\frac{x}{L}\right)^{n_x} \quad (2)$$

The $()_c$ and $()_m$ subscripts respectively denote the ceramic and metal, and n_R and n_x are FG power index along radius and length of tube, respectively, are related to the volume fraction change of the material composition and r is the distance from the center of the FG tube. The Young's modulus (E), Poisson's ratio (ν), shear modulus (G) and mass density (ρ) equations of the FG nanotube can be expressed as

$$E(r,x,T) = E_m + (E_c - E_m)\left(\frac{r - Ri}{Ro - Ri}\right)^{n_R}\left(\frac{x}{L}\right)^{n_x} - \frac{\alpha}{2}(E_c + E_m) \quad (3a)$$

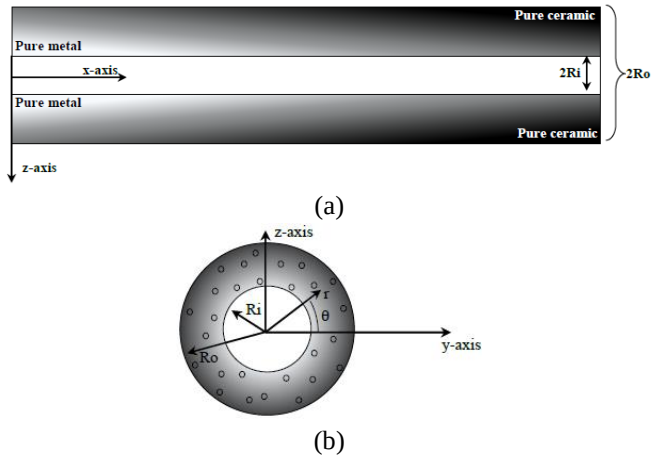

Fig. 1 Schematic of the studied structure

Table 1 Coefficients of Young's modulus, Poisson's ratio and mass density (Yang and Shen 2002)

	E (Pa)	ν	ρ (Kg/m^3)
SUS304	2.07787e11	0.3177	8166
Al_2O_3	3.23393e11	0.24	3800

$$\nu(r,x,T) = \nu_m + (\nu_c - \nu_m)\left(\frac{r-Ri}{Ro-Ri}\right)^{n_R}\left(\frac{x}{L}\right)^{n_x} - \frac{\alpha}{2}(\nu_c + \nu_m) \tag{3b}$$

$$G(r,x,T) = G_m + (G_c - G_m)\left(\frac{r-Ri}{Ro-Ri}\right)^{n_R}\left(\frac{x}{L}\right)^{n_x} - \frac{\alpha}{2}(G_c + G_m), \quad G = \frac{E}{2(1+\nu)} \tag{3c}$$

$$\rho(r,x,T) = \rho_m + (\rho_c - \rho_m)\left(\frac{r-Ri}{Ro-Ri}\right)^{n_R}\left(\frac{x}{L}\right)^{n_x} - \frac{\alpha}{2}(\rho_c + \rho_m) \tag{3d}$$

where α defines the porosity coefficient which is shown in Fig. 1(b).

2.2 Mathematical modeling

The boundary conditions and the governing equations are obtained by the Hamiltonian principle as below (Zhang *et al*. 2015, 2017, 2019, 2020, Ghadiri and Shafiei 2016, Ghadiri *et al*. 2016, 2017a, b, c, Wang *et al*. 2016, 2020, 2021, Ebrahimi *et al*. 2017, 2020a, b, Mirjavadi *et al*. 2017, Shafiei *et al*. 2017, 2019, Shivanian *et al*. 2017, Li *et al*. 2018, 2019, Chen *et al*. 2019, 2020, Gao *et al*. 2019, 2020a, b, Ghabussi *et al*. 2019, 2020, 2021, Moayedi *et al*. 2019, Cao 2020, Duan *et al*. 2020, 2021, Huang *et al*. 2020, Safarpour *et al*. 2020, Shariati *et al*. 2020a, b, Liu *et al*. 2021, Lu *et al*. 2021, Morasaei *et al*. 2021, Sui *et al*. 2021, Yin *et al*. 2021)

$$\int_{t_1}^{t_2} \delta H dt = \int_{t_1}^{t_2} (\delta S + \delta V) dt = 0 \tag{4}$$

S and V, respectively define the strain energy and external work. The displacement at any one point of the nanotube based on the beam model of tubes by the different tube model is

$$\begin{aligned} &u_1(x,y,z,t) \\ &= u - z\frac{\partial w(x,t)}{\partial x} + g(y,z)\left[\frac{\partial w(x,t)}{\partial x} + \psi(x,t)\right] \\ &u_2(x,y,z,t) = 0 \\ &u_3(x,y,z,t) = w(x,t) \end{aligned} \tag{5}$$

where u_1, u_2 and u_3 respectively are the components of displacement field along x, y and z directions and $\partial w/\partial x$ and w(x) denote the angle of rotation around the y axis and the transverse deflection of the nanotube respectively and ψ is rotation. In which

$$g(y,z) = z + z\left(R_0{}^2 R_i{}^2 r^{-2} - \frac{r^2}{3}\right)\left(R_0{}^2 + R_i{}^2\right)^{-1} \tag{6}$$

If we set g = z or g = 0, the present model will change to Timoshenko and Euler-Bernoulli beam models, respectively. This model yields more accurate results and fewer parameters comparing with the moderately thick shell and Timoshenko beam models. The strain energy of the FG tapered nanotube which results from the strains and stresses of the nanotube is defined as

$$\begin{aligned} S &= \iiint sdv \\ &= \frac{1}{2}\iiint \left(\sigma_{xx}\varepsilon_{xx} + 2\left(\sigma_{xy}\varepsilon_{xy} + \sigma_{xz}\varepsilon_{xz}\right)\right) dv \end{aligned} \tag{7}$$

On the basis of the assumption of large transverse displacements, moderate rotations and small strains for a straight Zhang-Fu's tube model, the strain-displacement relation is defined as

$$\varepsilon_{xx} = \frac{\partial u_1}{\partial x} = \frac{\partial u}{\partial x} - z\frac{\partial^2 w}{\partial x^2} + g(y,z)\left(\frac{\partial^2 w}{\partial x^2} + \frac{\partial \psi}{\partial x}\right) \tag{8a}$$

$$\varepsilon_{xy} = \frac{1}{2}\left(\frac{\partial u_1}{\partial y} + \frac{\partial u_2}{\partial x}\right) = \frac{1}{2}\frac{\partial g(y,z)}{\partial y}\left(\frac{\partial w}{\partial x} + \psi\right) \tag{8b}$$

$$\varepsilon_{xz} = \frac{1}{2}\left(\frac{\partial u_1}{\partial z} + \frac{\partial u_3}{\partial x}\right) = \frac{1}{2}\frac{\partial g(y,z)}{\partial z}\left(\frac{\partial w}{\partial x} + \psi\right) \tag{8c}$$

And stresses are

$$\sigma_{xx} = E\varepsilon_{xx} \tag{9a}$$

$$\sigma_{xy} = G\varepsilon_{xy}, \qquad G = \frac{E}{2(1+\nu)} \tag{9b}$$

$$\sigma_{xz} = G\varepsilon_{xy} \tag{9c}$$

The virtual strain energy of the FG tapered nanotube is defined as

$$\delta S = \iiint \delta s dv \tag{10}$$

$$= \int_0^L \begin{bmatrix} A_{11}\frac{\partial u}{\partial x}\delta\left(\frac{\partial u}{\partial x}\right) + D_{11}\frac{\partial^2 w}{\partial x^2}\delta\left(\frac{\partial^2 w}{\partial x^2}\right) \\ +H_{11}\left(\frac{\partial^2 w}{\partial x^2}\delta\left(\frac{\partial^2 w}{\partial x^2}\right) + \frac{\partial \psi}{\partial x}\delta\left(\frac{\partial \psi}{\partial x}\right) + \frac{\partial^2 w}{\partial x^2}\delta\left(\frac{\partial \psi}{\partial x}\right) + \frac{\partial \psi}{\partial x}\left(\frac{\partial^2 w}{\partial x^2}\right)\right) \\ \iint \begin{bmatrix} -z\frac{\partial^2 w}{\partial x^2}\delta\left(\frac{\partial u}{\partial x}\right) - z\frac{\partial u}{\partial x}\left(\frac{\partial^2 w}{\partial x^2}\right) + g\frac{\partial u}{\partial x}\delta\left(\frac{\partial^2 w}{\partial x^2}\right) \\ +g\frac{\partial^2 w}{\partial x^2}\delta\left(\frac{\partial u}{\partial x}\right) + g\frac{\partial u}{\partial x}\delta\left(\frac{\partial \psi}{\partial x}\right) + g\frac{\partial \psi}{\partial x}\delta\left(\frac{\partial \psi}{\partial x}\right) \end{bmatrix} dA \\ -2E_{11}\frac{\partial^2 w}{\partial x^2}\delta\left(\frac{\partial^2 w}{\partial x^2}\right) - E_{11}\frac{\partial^2 w}{\partial x^2}\delta\left(\frac{\partial \psi}{\partial x}\right) - E_{11}\frac{\partial \psi}{\partial x}\delta\left(\frac{\partial^2 w}{\partial x^2}\right) \\ +A_{11}\left(\frac{1}{2}\left(\frac{\partial w}{\partial x}\right)^3\delta\left(\frac{\partial w}{\partial x}\right) + \frac{\partial u}{\partial x}\frac{\partial w}{\partial x}\delta\left(\frac{\partial w}{\partial x}\right) + \frac{1}{2}\left(\frac{\partial w}{\partial x}\right)^2\delta\left(\frac{\partial u}{\partial x}\right)\right) \\ +B_{11}\left(\frac{\partial w}{\partial x}\delta\left(\frac{\partial w}{\partial x}\right) + \psi\delta(\psi) + \frac{\partial w}{\partial x}\delta(\psi) + \psi\delta\left(\frac{\partial w}{\partial x}\right)\right) \end{bmatrix} dx$$

where

$$(A_{11}, D_{11}, E_{11}, H_{11}) = \iint_A E(r,T)(1, z^2, zg, g^2)dA \quad (11a)$$

$$B_{11} = \iint_A G(r,T)\left[\left(\frac{\partial g}{\partial y}\right)^2 + \left(\frac{\partial g}{\partial z}\right)^2\right]dA \quad (11b)$$

The external work due to the applied buckling force (F) is

$$\delta V = \int_0^L F\frac{\partial w}{\partial x}\delta\left(\frac{\partial w}{\partial x}\right)dx \quad (12)$$

Substituting Eqs. (10) and (12) into Eq. (4) and setting the coefficients of δu, δw and δψ to zero, the following Euler–Lagrange equation can be obtained

$$\delta u: -\frac{\partial N_{xx}}{\partial x} = 0 \quad (13a)$$

$$\delta w: \frac{\partial^2 P}{\partial x^2} - \frac{\partial^2 M}{\partial x^2} - \frac{\partial Q}{\partial x} + \frac{\partial}{\partial x}\left(F\frac{\partial w}{\partial x}\right) = 0 \quad (13b)$$

$$\delta\psi: \frac{\partial P}{\partial x} - Q = 0 \quad (13c)$$

where

$$N_{xx} = A_{11}\frac{\partial u}{\partial x} \quad (14a)$$

$$P = H_{11}\left(\frac{\partial^2 w}{\partial x^2} + \frac{\partial \psi}{\partial x}\right) - E_{11}\frac{\partial^2 w}{\partial x^2} \quad (14b)$$

$$M = E_{11}\left(\frac{\partial^2 w}{\partial x^2} + \frac{\partial \psi}{\partial x}\right) - D_{11}\frac{\partial^2 w}{\partial x^2} \quad (14c)$$

$$Q = B_{11}\left(\frac{\partial w}{\partial x} + \psi\right) \quad (14d)$$

And boundary conditions are

$$u = 0 \text{ or } A_{11}\frac{\partial u}{\partial x} = 0 \quad (15a)$$

$$w = 0 \text{ or } \frac{\partial M}{\partial x} - \frac{\partial P}{\partial x} + Q = 0 \quad (15b)$$

$$\psi = 0 \text{ or } A_{11}\frac{\partial u}{\partial x} = 0 \quad (15c)$$

$$\frac{\partial w}{\partial x} = 0 \text{ or } M - P = 0 \quad (15d)$$

2.3 Nonlocal strain gradient theory

The nonlocal strain gradient theory (NSGT) proposed by Lim *et al*. (2015), based on the basic assumptions of NSGT, the total stress tensor t_{xx} is assumed to be of the form

$$[1 - (ea)^2\nabla^2]t_{xx} = E(1 - l^2\nabla^2)\varepsilon_{xx} \quad (16)$$

Here, ea is the nonlocal parameters, while l is strain gradient parameter, E is the Young's

modulus, L is the length of the nanotube. Where $\nabla^2 = d^2/dx^2$ is the Laplace operator. By using the nonlocal strain gradient theory equations, the stress resultants (Eq. (14)) can be rewriting as

$$N_{xx} = (ea)^2\frac{\partial^2 N_{xx}}{\partial x^2} + \left(1 - l^2\frac{d^2}{dx^2}\right)\left(A_{11}\frac{\partial u}{\partial x}\right) \quad (17a)$$

$$P = (ea)^2\frac{\partial^2 P}{\partial x^2} + \left(1 - l^2\frac{d^2}{dx^2}\right)\begin{bmatrix} H_{11}\left(\frac{\partial^2 w}{\partial x^2} + \frac{\partial \psi}{\partial x}\right) \\ -E_{11}\frac{\partial^2 w}{\partial x^2}\end{bmatrix} \quad (17b)$$

$$M = (ea)^2\frac{\partial^2 M}{\partial x^2} + \left(1 - l^2\frac{d^2}{dx^2}\right)\begin{bmatrix} E_{11}\left(\frac{\partial^2 w}{\partial x^2} + \frac{\partial \psi}{\partial x}\right) \\ -D_{11}\frac{\partial^2 w}{\partial x^2}\end{bmatrix} \quad (17c)$$

$$Q = (ea)^2\frac{\partial^2 Q}{\partial x^2} + \left(1 - l^2\frac{d^2}{dx^2}\right)\left[B_{11}\left(\frac{\partial w}{\partial x} + \psi\right)\right] \quad (17d)$$

Thus, the higher order Zhang-Fu's tube model defines the general equation of vibration of non-uniform FG nanotubes based on the nonlocal strain gradient theory as below

δu:

$$\begin{aligned} &\frac{dA_{11}(x)}{dx}\frac{\partial u}{\partial x} + A_{11}(x)\frac{\partial^2 u}{\partial x^2} \\ &-l^2\begin{bmatrix}\frac{d^3A_{11}(x)}{dx^3}\frac{\partial u}{\partial x} + 3\frac{d^2A_{11}(x)}{dx^2}\frac{\partial^2 u}{\partial x^2} \\ +3\frac{dA_{11}(x)}{dx}\frac{\partial^3 u}{\partial x^3} + A_{11}(x)\frac{\partial^4 u}{\partial x^4}\end{bmatrix} = 0 \end{aligned} \quad (18a)$$

δψ:

$$\begin{aligned} &\frac{dEE(x)}{dx}\frac{\partial^2 w}{\partial x^2} + EE(x)\frac{\partial^3 w}{\partial x^3} + \frac{dH_{11}(x)}{dx}\frac{\partial \psi}{\partial x} + H_{11}(x)\frac{\partial^2 \psi}{\partial x^2} \\ &\quad - B_{11}(x)\left(\frac{\partial w}{\partial x} + \psi\right) \\ &-l^2\begin{bmatrix}\frac{d^3EE(x)}{dx^3}\frac{\partial^2 w}{\partial x^2} + 3\frac{d^2EE(x)}{dx^2}\frac{\partial^3 w}{\partial x^3} + 3\frac{dEE(x)}{dx}\frac{\partial^4 w}{\partial x^4} + EE(x)\frac{\partial^5 w}{\partial x^5} \\ +\frac{d^3H_{11}(x)}{dx^3}\frac{\partial \psi}{\partial x} + 3\frac{d^2H_{11}(x)}{dx^2}\frac{\partial^2 \psi}{\partial x^2} + 3\frac{dH_{11}(x)}{dx}\frac{\partial^3 \psi}{\partial x^3} + H_{11}(x)\frac{\partial^4 \psi}{\partial x^4} \\ -\begin{pmatrix}B_{11}(x)\frac{\partial^3 w}{\partial x^3} + \frac{d^2B_{11}(x)}{dx^2}\frac{\partial w}{\partial x} + 2\frac{dB_{11}(x)}{dx}\frac{\partial^2 w}{\partial x^2} \\ +B_{11}(x)\frac{\partial^2 \psi}{\partial x^2} + \frac{d^2B_{11}(x)}{dx^2}\psi + 2\frac{dB_{11}(x)}{dx}\frac{\partial \psi}{\partial x}\end{pmatrix}\end{bmatrix} \\ &\quad = 0 \end{aligned} \quad (18b)$$

δw:

$$
\begin{aligned}
&E(x)\frac{\partial^4 w}{\partial x^4}+2\frac{dE(x)}{dx}\frac{\partial^3 w}{\partial x^3}+\frac{d^2E(x)}{dx^2}\frac{\partial^2 w}{\partial x^2}+\frac{d^2EE(x)}{dx^2}\frac{\partial \psi}{\partial x}+2\frac{dEE(x)}{dx}\frac{\partial^2 \psi}{\partial x^2}\\
&+EE(x)\frac{\partial^3 \psi}{\partial x^3}-\frac{dB_{11}(x)}{dx}\left(\frac{\partial w}{\partial x}+\psi\right)-B_{11}(x)\left(\frac{\partial^2 w}{\partial x^2}+\frac{\partial \psi}{\partial x}\right)\\
&-l^2\begin{bmatrix}E(x)\frac{\partial^6 w}{\partial x^6}+4\frac{dE(x)}{dx}\frac{\partial^5 w}{\partial x^5}+6\frac{d^2E(x)}{dx^2}\frac{\partial^4 w}{\partial x^4}+4\frac{d^3E(x)}{dx^3}\frac{\partial^3 w}{\partial x^3}+\frac{d^4E(x)}{dx^4}\frac{\partial^2 w}{\partial x^2}\\+\frac{d^4EE(x)}{dx^4}\frac{\partial \psi}{\partial x}+4\frac{d^3EE(x)}{dx^3}\frac{\partial^2 \psi}{\partial x^2}\\+6\frac{d^2EE(x)}{dx^2}\frac{\partial^3 \psi}{\partial x^3}+4\frac{dEE(x)}{dx}\frac{\partial^4 \psi}{\partial x^4}+EE(x)\frac{\partial^5 \psi}{\partial x^5}\\-\left(\frac{d^3B_{11}(x)}{dx^3}\frac{\partial w}{\partial x}+B_{11}(x)\frac{\partial^4 w}{\partial x^4}+3\frac{d^2B_{11}(x)}{dx^2}\frac{\partial^2 w}{\partial x^2}+3\frac{dB_{11}(x)}{dx}\frac{\partial^3 w}{\partial x^3}\right)\\-\left(B_{11}(x)\frac{\partial^3 \psi}{\partial x^3}+\frac{d^3B_{11}(x)}{dx^3}\psi+3\frac{dB_{11}(x)}{dx}\frac{\partial^2 \psi}{\partial x^2}+3\frac{d^2B_{11}(x)}{dx^2}\frac{\partial \psi}{\partial x}\right)\end{bmatrix}\\
&+F\frac{\partial^2 w}{\partial x^2}-(ea^2)\left(F\frac{\partial^4 w}{\partial x^4}\right)=0
\end{aligned}
\tag{18c}
$$

where

$$
\begin{aligned}
E(x)&=H_{11}(x)+D_{11}(x)-2E_{11}(x)\\
EE(x)&=H_{11}(x)-E_{11}(x)
\end{aligned}
\tag{19}
$$

3. Solution methodology

The results of this study are derived by solving the governing equations using the generalized differential quadrature method (GDQM) which defines the r-th order derivative of function f(x_i) as

$$
\left.\frac{\partial^r f(x)}{\partial x^r}\right|_{x=x_P}=\sum_{j=1}^{n}C_{ij}^{(r)}f(x_i) \tag{20}
$$

n is the grid points number along x direction and C_{ij} is

$$
\begin{aligned}
&C_{ij}^{(1)}=\frac{\widetilde{M}(x_i)}{(x_i-x_j)\widetilde{M}(x_j)};\\
&i,j=1,2,\dots,n\ and\ i\neq j\\
&C_{ij}^{(1)}=-\sum_{j=1,i\neq j}^{n}C_{ij}^{(1)};i=j
\end{aligned}
\tag{21}
$$

where $\widetilde{M}(x)$ is

$$
\widetilde{M}(x_i)=\prod_{j=1,j\neq i}^{n}(x_i-x_j) \tag{22}
$$

The weighting coefficient $C^{(r)}$, along x direction is derived as

$$
\begin{aligned}
&C_{ij}^{(r)}=r\left[C_{ij}^{(r-1)}C_{ij}^{(1)}-\frac{C_{ij}^{(r-1)}}{(x_i-x_j)}\right];\\
&i,\ j=1,2,\dots,n,i\neq j\ and\ 2\leq r\leq n-1\\
&C_{ii}^{(r)}=-\sum_{j=1,i\neq j}^{n}C_{ij}^{(r)};\\
&i,\ j=1,2,\dots,n\ and\ 1\leq r\leq n-1
\end{aligned}
\tag{23}
$$

Chebyshev-Gauss-Lobatto approach is employed to obtain the distribution of the mesh points as

$$
x_i=\frac{L}{2}\left(1-cos\left(\frac{(i-1)}{(N-1)}\pi\right)\right)i=1,2,3,\dots,n \tag{24}
$$

The motion equations and boundary conditions (Eqs. (15) and (18)) are assumed to be the combination of three matrixes. Then the linear stiffness matrix can be calculated as

$$
\{[K]-\omega^2[M]\}\{\lambda\}=0 \tag{25}
$$

The linear motion equation is first solved by GDQM and then, by employing the weight coefficients (Eq. (23)) to the linear motion equation we have

$$
\begin{aligned}
&\frac{dA_{11}(x)}{dx}\sum_{s=1}^{n}C_{rs}^{(1)}u_s+A_{11}(x)\sum_{s=1}^{n}C_{rs}^{(2)}u_s\\
&-l^2\begin{bmatrix}\frac{d^3A_{11}(x)}{dx^3}\sum_{s=1}^{n}C_{rs}^{(1)}u_s+3\frac{d^2A_{11}(x)}{dx^2}\sum_{s=1}^{n}C_{rs}^{(2)}u_s\\+3\frac{dA_{11}(x)}{dx}\sum_{s=1}^{n}C_{rs}^{(3)}u_s+A_{11}(x)\sum_{s=1}^{n}C_{rs}^{(4)}u_s\end{bmatrix}=0
\end{aligned}
\tag{26a}
$$

$$
\begin{aligned}
&\frac{dEE(x)}{dx}\sum_{s=1}^{n}C_{rs}^{(2)}w_s+EE(x)\sum_{s=1}^{n}C_{rs}^{(3)}w_s+\frac{dH_{11}(x)}{dx}\sum_{s=1}^{n}C_{rs}^{(1)}\psi_s\\
&+H_{11}(x)\sum_{s=1}^{n}C_{rs}^{(2)}\psi_s-B_{11}(x)\left(\sum_{s=1}^{n}C_{rs}^{(1)}w_s+\psi_s\right)\\
&-l^2\begin{bmatrix}\frac{d^3EE(x)}{dx^3}\sum_{s=1}^{n}C_{rs}^{(2)}w_s+3\frac{d^2EE(x)}{dx^2}\sum_{s=1}^{n}C_{rs}^{(3)}w_s+3\frac{dEE(x)}{dx}\sum_{s=1}^{n}C_{rs}^{(4)}w_s\\+EE(x)\sum_{s=1}^{n}C_{rs}^{(5)}w_s+\frac{d^3H_{11}(x)}{dx^3}\sum_{s=1}^{n}C_{rs}^{(1)}\psi_s+3\frac{d^2H_{11}(x)}{dx^2}\sum_{s=1}^{n}C_{rs}^{(2)}\psi_s\\+3\frac{dH_{11}(x)}{dx}\sum_{s=1}^{n}C_{rs}^{(3)}\psi_s+H_{11}(x)\sum_{s=1}^{n}C_{rs}^{(4)}\psi_s\\-\left(B_{11}(x)\sum_{s=1}^{n}C_{rs}^{(3)}w_s+\frac{d^2B_{11}(x)}{dx^2}\sum_{s=1}^{n}C_{rs}^{(1)}w_s+2\frac{dB_{11}(x)}{dx}\sum_{s=1}^{n}C_{rs}^{(2)}w_s\right)\\-\left(+B_{11}(x)\sum_{s=1}^{n}C_{rs}^{(2)}\psi_s+\frac{d^2B_{11}(x)}{dx^2}\psi_s+2\frac{dB_{11}(x)}{dx}\sum_{s=1}^{n}C_{rs}^{(1)}\psi_s\right)\end{bmatrix}\\
&=0
\end{aligned}
\tag{26b}
$$

$$
\begin{aligned}
&E(x)\sum_{s=1}^{n}C_{rs}^{(4)}w_s+2\frac{dE(x)}{dx}\sum_{s=1}^{n}C_{rs}^{(3)}w_s+\frac{d^2E(x)}{dx^2}\sum_{s=1}^{n}C_{rs}^{(2)}w_s\\
&+\frac{d^2EE(x)}{dx^2}\sum_{s=1}^{n}C_{rs}^{(1)}\psi_s+2\frac{dEE(x)}{dx}\sum_{s=1}^{n}C_{rs}^{(2)}\psi_s+EE(x)\sum_{s=1}^{n}C_{rs}^{(3)}\psi_s\\
&-\frac{dB_{11}(x)}{dx}\left(\sum_{s=1}^{n}C_{rs}^{(1)}w_s+\psi_s\right)-B_{11}(x)\left(\sum_{s=1}^{n}C_{rs}^{(2)}w_s+\sum_{s=1}^{n}C_{rs}^{(1)}\psi_s\right)\\
&-l^2\begin{bmatrix}E(x)\sum_{s=1}^{n}C_{rs}^{(6)}w_s+4\frac{dE(x)}{dx}\sum_{s=1}^{n}C_{rs}^{(5)}w_s+6\frac{d^2E(x)}{dx^2}\sum_{s=1}^{n}C_{rs}^{(4)}w_s\\+4\frac{d^3E(x)}{dx^3}\sum_{s=1}^{n}C_{rs}^{(3)}w_s+\frac{d^4E(x)}{dx^4}\sum_{s=1}^{n}C_{rs}^{(2)}w_s\\+\frac{d^4EE(x)}{dx^4}\sum_{s=1}^{n}C_{rs}^{(1)}\psi_s+4\frac{d^3EE(x)}{dx^3}\sum_{s=1}^{n}C_{rs}^{(2)}\psi_s+6\frac{d^2EE(x)}{dx^2}\sum_{s=1}^{n}C_{rs}^{(3)}\psi_s\\+4\frac{dEE(x)}{dx}\sum_{s=1}^{n}C_{rs}^{(4)}\psi_s+EE(x)\sum_{s=1}^{n}C_{rs}^{(5)}\psi_s\\-\left(\frac{d^3B_{11}(x)}{dx^3}\sum_{s=1}^{n}C_{rs}^{(1)}w_s+B_{11}(x)\sum_{s=1}^{n}C_{rs}^{(4)}w_s\right.\\\left.+3\frac{d^2B_{11}(x)}{dx^2}\sum_{s=1}^{n}C_{rs}^{(2)}w_s+3\frac{dB_{11}(x)}{dx}\sum_{s=1}^{n}C_{rs}^{(3)}w_s\right)\\-\left(B_{11}(x)\sum_{s=1}^{n}C_{rs}^{(3)}\psi_s+\frac{d^3B_{11}(x)}{dx^3}\psi_s+3\frac{dB_{11}(x)}{dx}\sum_{s=1}^{n}C_{rs}^{(2)}\psi_s\right.\\\left.+3\frac{d^2B_{11}(x)}{dx^2}\sum_{s=1}^{n}C_{rs}^{(1)}\psi_s\right)\end{bmatrix}\\
&=F\sum_{s=1}^{n}C_{rs}^{(2)}w_s-(ea^2)F\sum_{s=1}^{n}C_{rs}^{(4)}w_s=0
\end{aligned}
\tag{26c}
$$

Using the boundary conditions Eq. (15), and assembling the related matrixes to the boundary conditions and governing equations, the fundamental frequency of nanotubes can be obtained as below

$$\begin{bmatrix}[K_{dd}] & [K_{db}]\\ [K_{bd}] & [K_{bb}]\end{bmatrix}\begin{Bmatrix}\{\lambda_d\}\\ \{\lambda_b\}\end{Bmatrix} = \omega^2\begin{bmatrix}[M_{dd}] & [M_{db}]\\ [M_{bd}] & [M_{bb}]\end{bmatrix}\begin{Bmatrix}\{\lambda_d\}\\ \{\lambda_b\}\end{Bmatrix} \quad (27)$$

where b and d indexes denote the boundary and domain, respectively and λ is the mode shape.

4. Results

The results are obtained to focus on the buckling behavior of the 2D-FG porous nanotube under the effects of different parameters. The buckling load is obtained for various values of different parameters for fully clamped (C-C), simply supported-clamped (S.S.-C), and fully simply supported (simply supported) boundary conditions. The buckling load is represented as the non-dimensional value to help us to understand the results better. Non-dimensional parameters are as

$$\mu_{ea} = \frac{ea}{Ro_0} \quad (28a)$$

$$\mu_l = \frac{l}{Ro_0} \quad (28b)$$

$$\Gamma = \frac{FL^2}{D_{11}(atx = 0)} \quad (28c)$$

Where μ_{ea}, μ_l and Γ are the non-dimensional nonlocal parameter, non-dimensional gradient strain parameter and non-dimensional buckling load, respectively.

Validation of the results is illustrated in Table 2, which shows the buckling load for different values of ea and L/h based on different theories. It can be observed that the present results are very convergent to the results of (Reddy 2007).

Tables 3, 4, and 5 show the buckling load of the porous 2D-FG nanotube based on higher-order theory and Timoshenko theory for clamped (CC), clamped-simply supported (CS), and simply supported (SS) boundary conditions, respectively. It is recognized that the buckling load which is achieved by Timoshenko theory is a little higher than that obtained by higher-order theory, which is because the degree of freedom of the Timoshenko theory is higher than the higher-order theory. It is seen that the buckling load of porous 2D-FG nanotube rises with the strain gradient parameter and decreases with the nonlocal parameter. Also, the increment of the FG power indexes along length and radius reduces the buckling load. The effect of L/Ro_0 is also displayed in these tables, which illustrates that increment of L/Ro_0 enhances the buckling load except when $\mu_l = 1$ and $\mu_{ea} = 0$. It is also concluded from Tables 3, 4 and 5 that the buckling load of porous 2D-FG nanotubes when the boundary condition is clamped-simply supported is higher than simply supported and lower than clamped boundary conditions.

Figs. 2 and 3 confirm the buckling load of clamped, clamped-simply supported, and simply supported 2D-FG nanotubes versus μ_{ea} and μ_l, respectively. It is pointed that increment of μ_{ea}, n_X and n_R decrease the buckling load while increasing μ_1 increases the buckling load of the 2D-FG nanotube. It is because the nonlocal parameter and FG power indexes decrease the stiffness of the material, while the strain gradient parameter raises the stiffness (Shafiei and She 2018).

Fig. 5 points to the buckling load of the porous 2D-FG nanotube to show the effects of n_X and n_R separately for different boundary conditions. It is seen that increment of n_R reduces the effect of n_X, and vice versa. It is also shown that the buckling load of clamped-simply supported boundary conditions is higher than simply supported and lower than clamped boundary conditions.

Fig. 6 describes the buckling load versus the FG power index across the radius (n_R) for different values of the FG power index along with the length of tube (n_X) and different values of nonlocal and strain gradient parameters. It is seen that increment of FG power index along the x-axis or across the radius reduces the effect of the other. In addition, it can be deducted from Fig. 6 that the nonlocal value decreases the buckling load while the strain gradient increases the buckling load. This is because the stiffness of the nanotube decreases by enhancing the nonlocal parameter, and on the other hand, the strain gradient parameter increases the stiffness of the nanotube (Shafiei and She 2018).

Table 2 Comparison of the results with Reddy (2007) for different theories

		L/h = 10	L/h = 20	L/h = 100
$(ea)^2 = 0.5$	Timoshenko Theory (Reddy 2007)	9.1701	9.3455	9.4031
	Euler-Bernoulli theory (Reddy 2007)	9.4055	9.4055	9.4055
	Reddy Theory (Reddy 2007)	9.1702	9.3455	9.4031
	Present higher order theory	9.16365074	9.33435821	9.40114819
	Present Timoshenko theory	9.15311629	9.32864207	9.40007257
$(ea)^2 = 2$	Timoshenko Theory (Reddy 2007)	8.0364	8.1900	8.2405
	Euler-Bernoulli theory (Reddy 2007)	8. 2426	8.2426	8.2426
	Reddy Theory (Reddy 2007)	8.0364	8.1900	8.2405
	Present higher order theory	8.03435821	8.18810943	8.23767307
	Present Timoshenko theory	8.03164207	8.17942475	8.23314235
$(ea)^2 = 4$	Timoshenko Theory (Reddy 2007)	6.8990	7.0310	7.0743
	Euler-Bernoulli theory (Reddy 2007)	7.0761	9.0761	7.0761
	Reddy Theory (Reddy 2007)	6.8991	7.0310	7.0743
	Present higher order theory	6.88514819	7.030686553	7.07404010
	Present Timoshenko theory	6.87987257	7.030194310	7.07390896

Table 3 Buckling load of FG and 2D-FG porous nanotubes for clamped supported boundary condition when $Ro_0 = 10Ri_0 = 1$ (nm), $\alpha = 0.05$

			$\mu_l = 0, \mu_{ea} = 0$	$\mu_l = 1, \mu_{ea} = 0$	$\mu_l = 0, \mu_{ea} = 1$	$\mu_l = 1, \mu_{ea} = 2$	$\mu_l = 2, \mu_{ea} = 3$
$\frac{L}{Ro_0} = 25$	$n_X = 1, n_R = 0$	Higher order Theory	29.51557	31.4581	27.75108	25.09944	23.7998
		Timoshenko	29.98132	31.95198	28.202	25.53733	24.26187
	$n_X = 0, n_R = 1$	Higher order Theory	32.92517	35.00491	30.969	27.94442	26.31223
		Timoshenko	33.25896	35.35978	31.28296	28.22772	26.57732
	$n_X = n_R = 1$	Higher order Theory	27.68564	29.46831	26.02818	23.49375	22.20135
		Timoshenko	28.12597	29.94357	26.45023	23.90151	22.61926
$\frac{L}{Ro_0} = 50$	$n_X = 1, n_R = 0$	Higher order Theory	30.57302	31.07417	30.09569	29.2217	28.51524
		Timoshenko	30.87978	31.38614	30.40082	29.52715	28.82688
	$n_X = 0, n_R = 1$	Higher order Theory	34.25464	34.79557	33.72212	32.72827	31.88656
		Timoshenko	34.34453	34.88688	33.81061	32.81415	31.97024
	$n_X = n_R = 1$	Higher order Theory	28.74962	29.21184	28.29976	27.4659	26.7719
		Timoshenko	29.00955	29.47778	28.55768	27.72392	27.0372
$\frac{L}{Ro_0} = 100$	$n_X = 1, n_R = 0$	Higher order Theory	30.85024	30.97656	30.72846	30.49325	30.2761
		Timoshenko	31.11324	31.24073	30.99121	30.7564	30.54139
	$n_X = 0, n_R = 1$	Higher order Theory	34.60418	34.74079	34.46811	34.20072	33.94456
		Timoshenko	34.62708	34.76379	34.49092	34.22335	33.96703
	$n_X = n_R = 1$	Higher order Theory	29.02893	29.14557	28.91406	28.68969	28.47749
		Timoshenko	29.23935	29.35731	29.12417	28.90017	28.69028

Table 4 Buckling load of FG and 2D-FG porous nanotubes for clamped-simply supported boundary condition when $Ro_0 = 10Ri_0 = 1$ (nm), $\alpha = 0.05$

			$\mu_l = 0, \mu_{ea} = 0$	$\mu_l = 1, \mu_{ea} = 0$	$\mu_l = 0, \mu_{ea} = 1$	$\mu_l = 1, \mu_{ea} = 2$	$\mu_l = 2, \mu_{ea} = 3$
$\frac{L}{Ro_0} = 25$	$n_X = 1, n_R = 0$	Higher order Theory	16.33447	16.93376	15.81991	14.98564	14.50053
		Timoshenko	16.77081	17.39699	16.24571	15.40763	14.94363
	$n_X = 0, n_R = 1$	Higher order Theory	17.21703	17.77129	16.68007	15.74396	15.06834
		Timoshenko	17.32971	17.8883	16.78856	15.84531	15.16445
	$n_X = n_R = 1$	Higher order Theory	14.97683	15.49614	14.50505	13.71178	13.19612
		Timoshenko	15.40917	15.95878	14.92538	14.12764	13.63735
$\frac{L}{Ro_0} = 50$	$n_X = 1, n_R = 0$	Higher order Theory	16.66624	16.81854	16.53187	16.28901	16.09826
		Timoshenko	17.05325	17.21208	16.91659	16.67342	16.49028
	$n_X = 0, n_R = 1$	Higher order Theory	17.61984	17.76202	17.4788	17.20664	16.95708
		Timoshenko	17.64916	17.79162	17.50784	17.23514	16.9851
	$n_X = n_R = 1$	Higher order Theory	15.30469	15.43719	15.18117	14.9506	14.75429
		Timoshenko	15.68096	15.82064	15.55489	15.32383	15.13577
$\frac{L}{Ro_0} = 100$	$n_X = 1, n_R = 0$	Higher order Theory	16.75136	16.7896	16.7174	16.65424	16.60075
		Timoshenko	17.12538	17.16523	17.09086	17.02769	16.97627
	$n_X = 0, n_R = 1$	Higher order Theory	17.72347	17.75924	17.68776	17.61699	17.54777
		Timoshenko	17.73087	17.76666	17.69515	17.62434	17.55509
	$n_X = n_R = 1$	Higher order Theory	15.3889	15.4222	15.35766	15.29772	15.24301
		Timoshenko	15.75043	15.78549	15.71857	15.65856	15.60606

Table 5 Buckling load of FG and 2D-FG porous nanotubes for simply supported boundary condition when $Ro_0 = 10Ri_0 = 1$ (nm), $\alpha = 0.05$

			$\mu_l = 0, \mu_{ea} = 0$	$\mu_l = 1, \mu_{ea} = 0$	$\mu_l = 0, \mu_{ea} = 1$	$\mu_l = 1, \mu_{ea} = 2$	$\mu_l = 2, \mu_{ea} = 3$
$\frac{L}{Ro_0} = 25$	$n_X = 1, n_R = 0$	Higher order Theory	7.770923	7.899309	7.64846	7.424551	7.246025
		Timoshenko	7.880449	8.011023	7.756725	7.531318	7.353298
	$n_X = 0, n_R = 1$	Higher order Theory	8.56366	8.698892	8.43053	8.182068	7.971619
		Timoshenko	8.586132	8.721719	8.452653	8.203539	7.992472
	$n_X = n_R = 1$	Higher order Theory	7.24239	7.358555	7.128639	6.917355	6.741389
		Timoshenko	7.335152	7.453805	7.220135	7.007695	6.833334
$\frac{L}{Ro_0} = 50$	$n_X = 1, n_R = 0$	Higher order Theory	7.844427	7.876823	7.813183	7.752861	7.697396
		Timoshenko	7.942101	7.974985	7.910584	7.849937	7.794595
	$n_X = 0, n_R = 1$	Higher order Theory	8.651045	8.685198	8.617027	8.550179	8.48614
		Timoshenko	8.656771	8.690947	8.62273	8.555838	8.491756
	$n_X = n_R = 1$	Higher order Theory	7.313827	7.343156	7.28478	7.227897	7.173886
		Timoshenko	7.394254	7.424151	7.364938	7.307825	7.25421
$\frac{L}{Ro_0} = 100$	$n_X = 1, n_R = 0$	Higher order Theory	7.863024	7.871142	7.855173	7.839802	7.825132
		Timoshenko	7.957666	7.965902	7.949749	7.934301	7.919661
	$n_X = 0, n_R = 1$	Higher order Theory	8.673174	8.681735	8.664623	8.647595	8.630751
		Timoshenko	8.674613	8.683174	8.66606	8.649029	8.632182
	$n_X = n_R = 1$	Higher order Theory	7.33191	7.33926	7.324609	7.310117	7.295877
		Timoshenko	7.409179	7.416668	7.401814	7.387269	7.373126

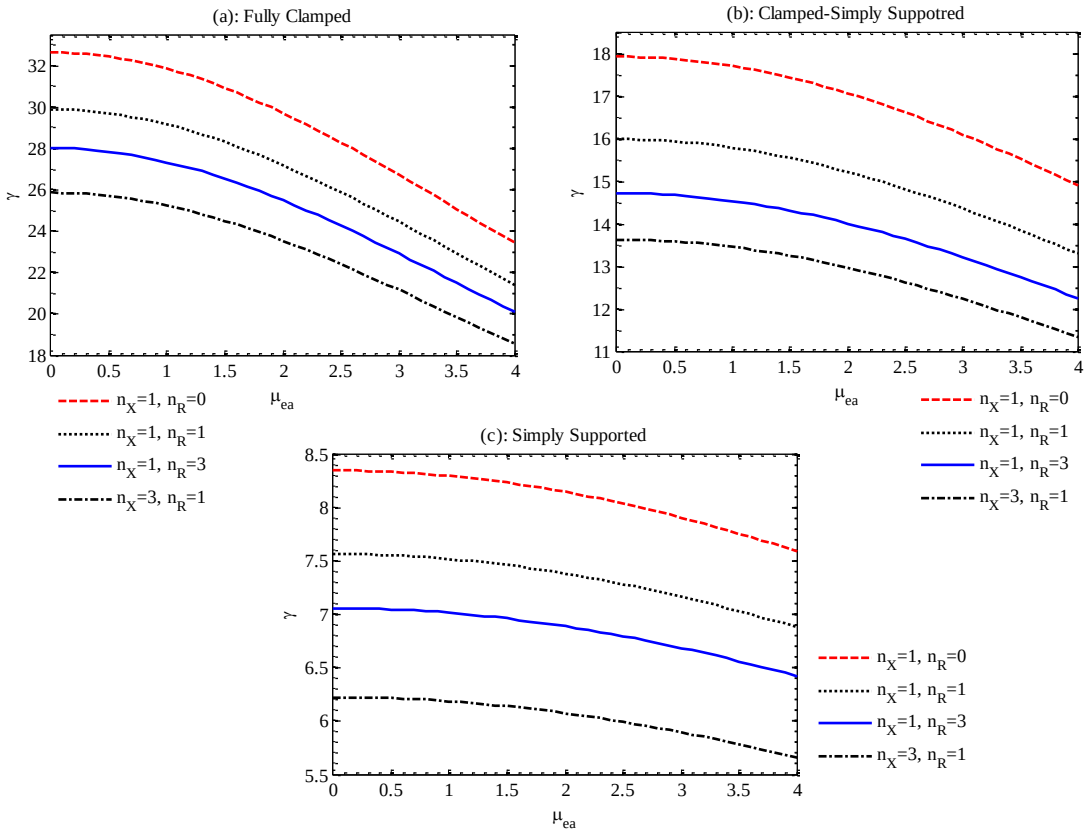

Fig. 2 Buckling load of 2D-FG perfect nanotube versus the nonlocal parameter (μ_{ea}) Ro = 2Ri = L/40 = 1 (nm), $\mu_l = 0.75$

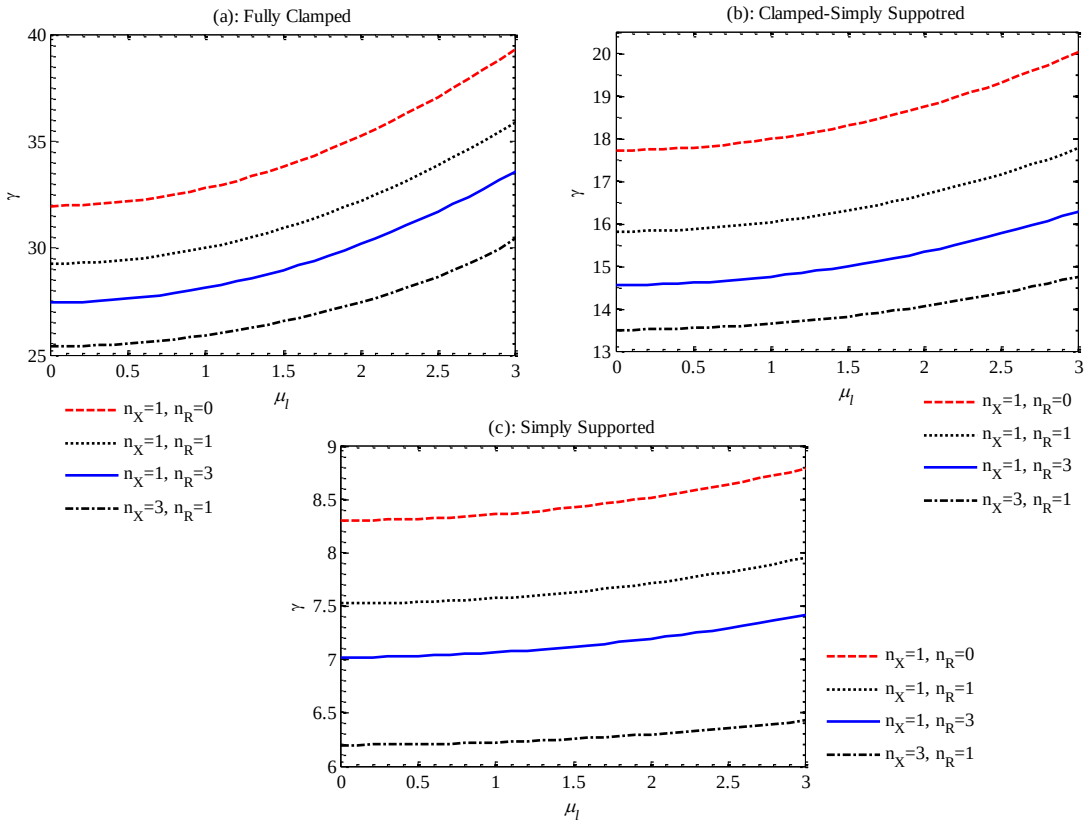

Fig. 3 Buckling load of 2D-FG perfect nanotube versus the strain gradient parameter (μ_l) when Ro = 2Ri = L/40 = 1 (nm), μ_{ea} = 0.75

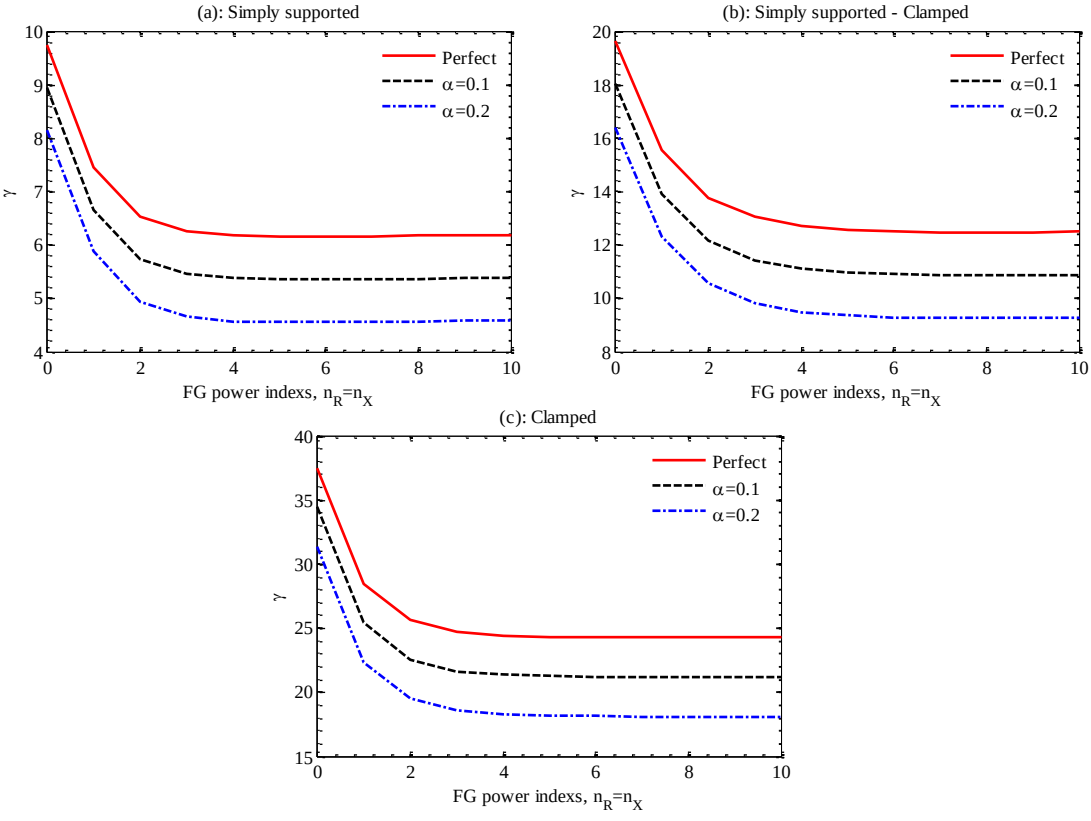

Fig. 4 Buckling load of 2D-FG porous and perfect nanotubes versus FG power indexes when Ro = 2Ri = L/40 = 1 (nm), μ_{ea} = 2, μ_l = 1

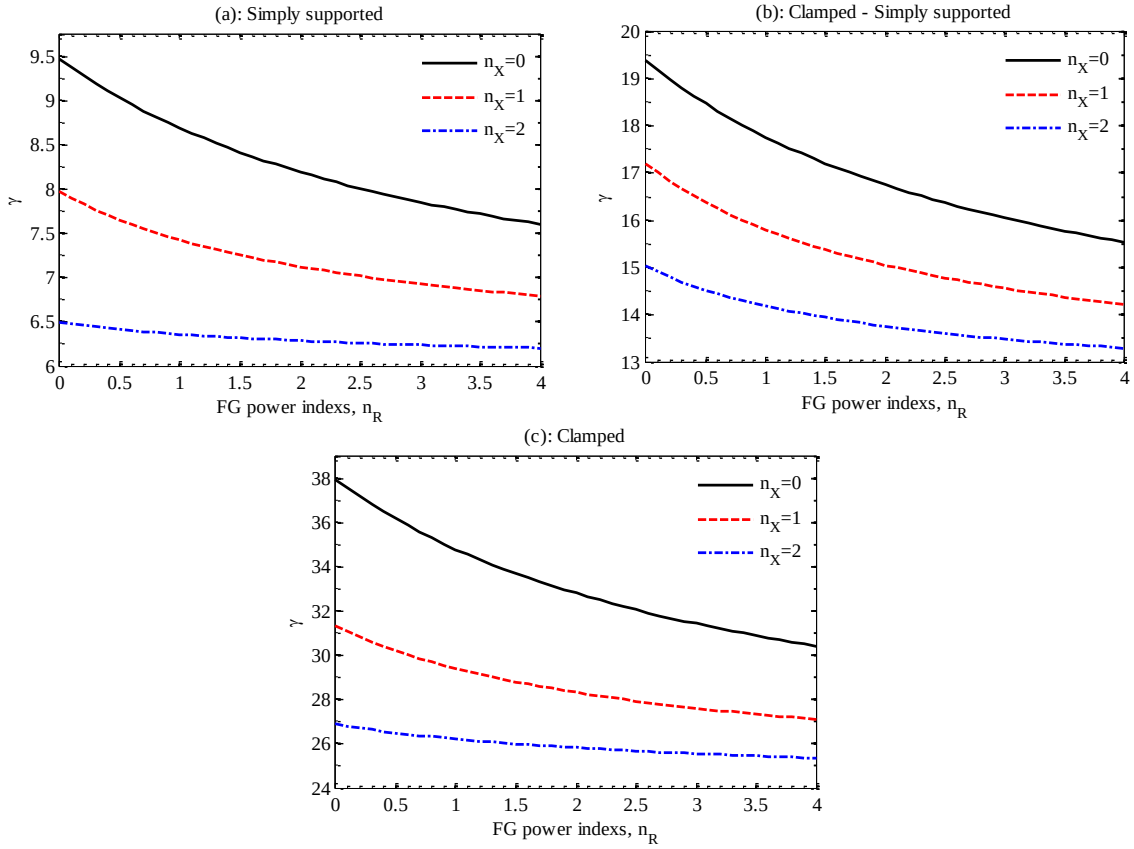

Fig. 5 Buckling load of 2D-FG porous nanotube versus n_R when Ro = 10Ri = L/40 = 1 (nm), $\mu_l = 2\mu_{ea} = 1$, $\alpha = 0.05$

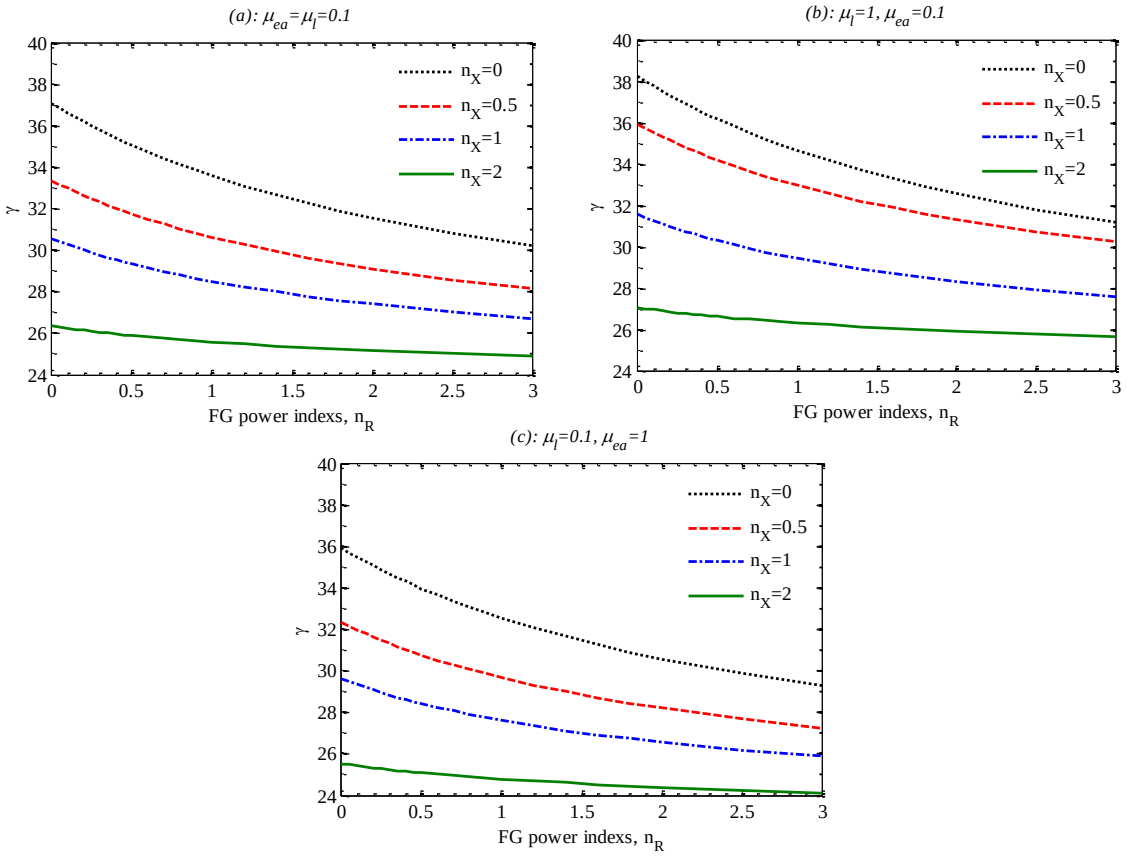

Fig. 6 Buckling load of 2D-FG porous clamped nanotube versus n_R when Ro = 5Ri = L/35 = 1 (nm), $\alpha = 0.05$

5. Conclusions

The investigation on buckling characteristics of two-dimensional functionally graded (2D-FG) imperfect nanotubes with porosity was presented in the present paper. Zhang-Fu's tube model is the basis of the nanotube model, and the nano-size effect is taken into attention by nonlocal and also strain gradient theories. The results are obtained employing GDQM, and the results are presented to show the effects of L/Ro_0, FG power indexes (n_X and n_R), nonlocal parameter, and strain gradient parameter. The main important results of this examination are as below

• The buckling load in the Timoshenko model is a little higher than the higher-order theory since the degree of freedom of Timoshenko theory is lower than that of the higher-order theory.

• The nonlocal parameter (μ_{ea}) decreases the buckling load due to reduces stiffness.

• The buckling load raises with the gradient strain parameter (μ_l) because the gradient strain enhances the strength of the tube.

• Both FG power indexes along the length (n_x) and along the radius (n_R) lead to decreases in the stiffness of tubes, and it means the reduces the buckling load; moreover, for a higher-value of four (n_x = 4 or n_R = 4), the influence of them is negligible.

• Growing the aspect ratio (L/Ro_0) leads to the increment of the buckling load. In contrast, the impact of aspect ratio is remarked to be different when μ_l = 1 and μ_{ea} = 0.

References

Aifantis, E.C. (1992), "On the role of gradients in the localization of deformation and fracture", *Int. J. Eng. Sci.*, **30**(10), 1279-1299. https://doi.org/10.1016/0020-7225(92)90141-3.

Akbas, S.D. (2018), "Forced vibration analysis of cracked functionally graded microbeams", *Adv. Nano Res., Int. J.*, **6**(1), 39-55. http://doi.org/10.12989/anr.2018.6.1.039.

Al-Furjan, M.S.H., Habibi, M., Rahimi, A., Chen, G., Safarpour, H., Safarpour, M. and Tounsi, A. (2020a), "Chaotic simulation of the multi-phase reinforced thermo-elastic disk using GDQM", *Eng. Comput.* https://doi.org/10.1007/s00366-020-01144-2.

Al-Furjan, M.S.H., Safarpour, H., Habibi, M., Safarpour, M. and Tounsi, A. (2020b), "A comprehensive computational approach for nonlinear thermal instability of the electrically FG-GPLRC disk based on GDQ method", *Eng. Comput.* https://doi.org/10.1007/s00366-020-01088-7.

Alipour, M., Torabi, M.A., Sareban, M., Lashini, H., Sadeghi, E., Fazaeli, A., Habibi, M. and Hashemi, R. (2020), "Finite element and experimental method for analyzing the effects of martensite morphologies on the formability of DP steels", *Mech. Based Des. Struct.*, **48**(5), 525-541. https://doi.org/10.1080/15397734.2019.1633343.

Amiri, A., Mohammadimehr, M. and Anvari, M. (2020), "Stress and buckling analysis of a thick-walled micro sandwich panel with a flexible foam core and carbon nanotube reinforced composite (CNTRC) face sheets", *Appl. Math. Mech.*, **41**(7), 1027-1038. https://doi.org/10.1007/s10483-020-2627-7.

Arshid, E., Arshid, H., Amir, S. and Mousavi, S.B. (2021), "Free vibration and buckling analyses of FG porous sandwich curved microbeams in thermal environment under magnetic field based on modified couple stress theory", *Arch. Civil Mech. Eng.*, **21**(1), 6. https://doi.org/10.1007/s43452-020-00150-x.

Aydogdu, M., Arda, M. and Filiz, S. (2018), "Vibration of axially functionally graded nano rods and beams with a variable nonlocal parameter", *Adv. Nano Res., Int. J.*, **6**(3), 257-278. http://doi.org/10.12989/anr.2018.6.3.257.

Azimi, M., Mirjavadi, S.S., Shafiei, N. and Hamouda, A.M.S. (2016), "Thermo-mechanical vibration of rotating axially functionally graded nonlocal Timoshenko beam", *Appl. Phys. A.*, **123**(1), 104. https://doi.org/10.1007/s00339-016-0712-5.

Bendaho, B., Belabed, Z., Bourada, M., Benatta, M.A., Bourada, F. and Tounsi, A. (2019), "Assessment of new 2D and quasi-3D Nonlocal theories for free vibration analysis of size-dependent functionally graded (FG) nanoplates", *Adv. Nano Res., Int. J.*, **7**(4), 277-292. https://doi.org/10.12989/anr.2019.7.4.277.

Bensattalah, T., Bouakkaz, K., Zidour, M. and Daouadji, T.H. (2018), "Critical buckling loads of carbon nanotube embedded in Kerr's medium", *Adv. Nano Res., Int. J.*, **6**(4), 339-356. http://doi.org/10.12989/anr.2018.6.4.339.

Bensattalah, T., Hamidi, A., Bouakkaz, K., Zidour, M. and Daouadji, T.H. (2020), "Critical buckling load of triple-walled carbon nanotube based on nonlocal elasticity theory", *J. Nano Res.*, **62**, 108-119. https://doi.org/10.4028/www.scientific.net/JNanoR.62.108.

Berghouti, H., Adda Bedia, E., Benkhedda, A. and Tounsi, A. (2019), "Vibration analysis of nonlocal porous nanobeams made of functionally graded material", *Adv. Nano Res., Int. J.*, **7**(5), 351-364. http://doi.org/10.12989/anr.2019.7.5.337.

Besseghier, A., Heireche, H., Bousahla, A.A., Tounsi, A. and Benzair, A. (2015), "Nonlinear vibration properties of a zigzag single-walled carbon nanotube embedded in a polymer matrix", *Adv. Nano Res., Int. J.*, **3**(1), 29-37. http://doi.org/10.12989/anr.2015.3.1.029.

Bian, L.C. and Wang, Y.W. (2020), "Temperature-related study on buckling properties of double-walled carbon nanotubes", *Eur. J. Mech.-A*, **80**, 103875. https://doi.org/10.1016/j.euromechsol.2019.103875.

Bravo, I., García-Mendiola, T., Revenga-Parra, M., Pariente, F. and Lorenzo, E. (2015), "Diazonium salt click chemistry based multiwall carbon nanotube electrocatalytic platforms", *Sensor. Actuat. B-Chem.*, **211**, 559-568. https://doi.org/10.1016/j.snb.2015.01.076.

Cao, L. (2020), "Changing port governance model: Port spatial structure and trade efficiency", *J. Coastal Res.*, **95**(SI), 963-968. https://doi.org/10.2112/si95-187.1.

Chemi, A., Heireche, H., Zidour, M., Rakrak, K. and Bousahla, A.A. (2015), "Critical buckling load of chiral double-walled carbon nanotube using non-local theory elasticity", *Adv. Nano Res., Int. J.*, **3**(4), 193-206. http://doi.org/10.12989/anr.2015.3.4.193.

Chen, X., Wang, D., Wang, T., Yang, Z., Zou, X., Wang, P., Luo, W., Li, Q., Liao, L., Hu, W. and Wei, Z. (2019), "Enhanced photoresponsivity of a GaAs nanowire metal-semiconductor-metal photodetector by adjusting the fermi level", *ACS Appl. Mater. Interf.*, **11**(36), 33188-33193. https://doi.org/10.1021/acsami.9b07891.

Chen, C., Wang, X., Wang, Y., Yang, D., Yao, F., Zhang, W., Wang, B., Sewvandi, G.A., Yang, D. and Hu, D. (2020), "Additive manufacturing of piezoelectric materials", *Adv. Funct. Mater.*, **30**(52), 2005141. https://doi.org/10.1002/adfm.202005141.

Duan, Z., Li, C., Zhang, Y., Dong, L., Bai, X., Yang, M., Jia, D., Li, R., Cao, H. and Xu, X. (2020a), "Milling surface roughness for 7050 aluminum alloy cavity influenced by nozzle position of nanofluid minimum quantity lubrication", *Chinese J. Aeronaut.*, https://doi.org/10.1016/j.cja.2020.04.029.

Duan, Z., Yin, Q., Li, C., Dong, L., Bai, X., Zhang, Y., Yang, M., Jia, D., Li, R. and Liu, Z. (2020b), "Milling force and surface morphology of 45 steel under different Al2O3 nanofluid concentrations", *Int. J. Adv. Manuf. Tech.*, **107**(3), 1277-1296. https://doi.org/10.1007/s00170-020-04969-9.

Duan, Z., Li, C., Ding, W., Zhang, Y., Yang, M., Gao, T., Cao, H., Xu, X., Wang, D., Mao, C., Li, H.N., Kumar, G.M., Said, Z., Debnath, S., Jamil, M. and Ali, H.M. (2021), "Milling force model for aviation aluminum alloy: Academic insight and perspective analysis", *Chinese J. Mech. Eng.*, **34**(1), 18. https://doi.org/10.1186/s10033-021-00536-9.

Ebrahimi, F. and Barati, M.R. (2019), "On static stability of electro-magnetically affected smart magneto-electro-elastic nanoplates", *Adv. Nano Res., Int. J.*, **7**(1), 63-75. http://doi.org/10.12989/anr.2019.7.1.063.

Ebrahimi, F., Shafiei, N., Kazemi, M. and Mousavi Abdollahi, S.M. (2017), "Thermo-mechanical vibration analysis of rotating nonlocal nanoplates applying generalized differential quadrature method", *Mech. Adv. Mater. Struct.*, **24**(15), 1257-1273. https://doi.org/10.1080/15376494.2016.1227499.

Ebrahimi, F., Hashemabadi, D., Habibi, M. and Safarpour, H. (2020a), "Thermal buckling and forced vibration characteristics of a porous GNP reinforced nanocomposite cylindrical shell", *Microsys. Technol.*, **26**(2), 461-473. https://doi.org/10.1007/s00542-019-04542-9.

Ebrahimi, F., Supeni, E.E.B., Habibi, M. and Safarpour, H. (2020b), "Frequency characteristics of a GPL-reinforced composite microdisk coupled with a piezoelectric layer", *Eur. Phys. J. Plus*, **135**(2), 144. https://doi.org/10.1140/epjp/s13360-020-00217-x.

Ehyaei, J., Akbarshahi, A. and Shafiei, N. (2017), "Influence of porosity and axial preload on vibration behavior of rotating FG nanobeam", *Adv. Nano Res., Int. J.*, **5**(2), 141-169. http://doi.org/10.12989/anr.2017.5.2.141.

Elmerabet, A.H., Heireche, H., Tounsi, A. and Semmah, A. (2017), "Buckling temperature of a single-walled boron nitride nanotubes using a novel nonlocal beam model", *Adv. Nano Res., Int. J.*, **5**(1), 1-12. http://doi.org/10.12989/anrr.2017.5.1.001.

Eltaher, M., Khater, M., Park, S., Abdel-Rahman, E. and Yavuz, M. (2016), "On the static stability of nonlocal nanobeams using higher-order beam theories", *Adv. Nano Res., Int. J.*, **4**(1), 51-64. http://doi.org/10.12989/anr.2016.4.1.051.

Eltaher, M.A., Almalki, T.A., Ahmed, K.I. and Almitani, K.H. (2019), "Characterization and behaviors of single walled carbon nanotube by equivalent-continuum mechanics approach", *Adv. Nano Res., Int. J.*, **7**(1), 39-49. http://doi.org/10.12989/anr.2019.7.1.039.

Eringen, A.C. (1983), "On differential equations of nonlocal elasticity and solutions of screw dislocation and surface waves", *J. Appl. Phys.*, **54**(9), 4703-4710. https://doi.org/10.1063/1.332803.

Esmailpoor Hajilak, Z., Pourghader, J., Hashemabadi, D., Sharifi Bagh, F., Habibi, M. and Safarpour, H. (2019), "Multilayer GPLRC composite cylindrical nanoshell using modified strain gradient theory", *Mech. Based Des. Struct.*, **47**(5), 521-545. https://doi.org/10.1080/15397734.2019.1566743.

Foroutan, K., Carrera, E. and Ahmadi, H. (2021), "Nonlinear hygrothermal vibration and buckling analysis of imperfect FG-CNTRC cylindrical panels embedded in viscoelastic foundations", *Eur. J. Mech.-A.*, **85**, 104107. https://doi.org/10.1016/j.euromechsol.2020.104107.

Gao, T., Li, C., Zhang, Y., Yang, M., Jia, D., Jin, T., Hou, Y. and Li, R. (2019), "Dispersing mechanism and tribological performance of vegetable oil-based CNT nanofluids with different surfactants", *Tribol. Int.*, **131**, 51-63. https://doi.org/10.1016/j.triboint.2018.10.025.

Gao, T., Li, C., Jia, D., Zhang, Y., Yang, M., Wang, X., Cao, H., Li, R., Ali, H.M. and Xu, X. (2020a), "Surface morphology assessment of CFRP transverse grinding using CNT nanofluid minimum quantity lubrication", *J. Clean. Prod.*, **277**, 123328. https://doi.org/10.1016/j.jclepro.2020.123328.

Gao, T., Zhang, X., Li, C., Zhang, Y., Yang, M., Jia, D., Ji, H., Zhao, Y., Li, R., Yao, P. and Zhu, L. (2020b), "Surface morphology evaluation of multi-angle 2D ultrasonic vibration integrated with nanofluid minimum quantity lubrication grinding", *J. Manuf. Process.*, **51**, 44-61. https://doi.org/10.1016/j.jmapro.2020.01.024.

García-Macías, E., Rodriguez-Tembleque, L., Castro-Triguero, R. and Sáez, A. (2017), "Buckling analysis of functionally graded carbon nanotube-reinforced curved panels under axial compression and shear", *Compos. Part B-Eng.*, **108**, 243-256. https://doi.org/10.1016/j.compositesb.2016.10.002.

Genoese, A., Genoese, A. and Salerno, G. (2020), "Buckling and post-buckling analysis of single wall carbon nanotubes using molecular mechanics", *Appl. Math. Model.*, **83**, 777-800. https://doi.org/10.1016/j.apm.2020.03.012.

Ghabussi, A., Ashrafi, N., Shavalipour, A., Hosseinpour, A., Habibi, M., Moayedi, H., Babaei, B. and Safarpour, H. (2019), "Free vibration analysis of an electro-elastic GPLRC cylindrical shell surrounded by viscoelastic foundation using modified length-couple stress parameter", *Mech. Based Des. Struct.*, 1-25. https://doi.org/10.1080/15397734.2019.1705166.

Ghabussi, A., Asgari Marnani, J. and Rohanimanesh, M.S. (2020a), "Improving seismic performance of portal frame structures with steel curved dampers", *Structures*, **24**, 27-40. https://doi.org/10.1016/j.istruc.2019.12.025.

Ghabussi, A., Habibi, M., NoormohammadiArani, O., Shavalipour, A., Moayedi, H. and Safarpour, H. (2020b), "Frequency characteristics of a viscoelastic graphene nanoplatelet–reinforced composite circular microplate", *J. Vib. Control*, **27**(1-2), 101-118. https://doi.org/10.1177/1077546320923930.

Ghabussi, A., Habibi, M., NoormohammadiArani, O., Shavalipour, A., Moayedi, H. and Safarpour, H. (2021), "Frequency characteristics of a viscoelastic graphene nanoplatelet–reinforced composite circular microplate", *J. Vib. Control*, **27**(1-2), 101-118. https://doi.org/10.1177/1077546320923930.

Ghadiri, M. and Shafiei, N. (2016), "Vibration analysis of a nano-turbine blade based on Eringen nonlocal elasticity applying the differential quadrature method", *J. Vib. Control*, **23**(19), 3247-3265. https://doi.org/10.1177/1077546315627723.

Ghadiri, M., Shafiei, N. and Alireza Mousavi, S. (2016), "Vibration analysis of a rotating functionally graded tapered microbeam based on the modified couple stress theory by DQEM", *Appl. Phys. A.*, **122**(9), 837. https://doi.org/10.1007/s00339-016-0364-5.

Ghadiri, M., Shafiei, N. and Alavi, H. (2017a), "Thermo-mechanical vibration of orthotropic cantilever and propped cantilever nanoplate using generalized differential quadrature method", *Mech. Adv. Mater. Struct.*, **24**(8), 636-646. https://doi.org/10.1080/15376494.2016.1196770.

Ghadiri, M., Shafiei, N. and Babaei, R. (2017b), "Vibration of a rotary FG plate with consideration of thermal and Coriolis effects", *Steel. Compos. Struct., Int. J.*, **25**(2), 197-207. https://doi.org/10.12989/SCS.2017.25.2.197.

Ghadiri, M., Shafiei, N. and Hossein, A.S. (2017c), "Vibration analysis of a rotating nanoplate using nonlocal elasticity theory", *J. Solid Mech.*, **9**(2), 319-337.

Goel, M., Harsha, S.P., Mishra, M.P. and Mishra, R.K. (2020), "Buckling failure analysis of defective carbon nanotubes using molecular dynamics simulation", *J. Fail. Anal. Prev.*, **20**(3), 868-881. https://doi.org/10.1007/s11668-020-00886-x.

Habibi, M., Hashemi, R., Sadeghi, E., Fazaeli, A., Ghazanfari, A. and Lashini, H. (2016), "Enhancing the mechanical properties and formability of low carbon steel with dual-phase microstructures", *J. Mater. Eng. Perform.*, **25**(2), 382-389. https://doi.org/10.1007/s11665-016-1882-1.

Huang, B., Li, C., Zhang, Y., Ding, W., Yang, M., Yang, Y., Zhai, H., Xu, X., Wang, D., Debnath, S., Jamil, M., Li, H.N., Ali, H.M., Gupta, M.K. and Said, Z. (2020), "Advances in fabrication of ceramic corundum abrasives based on sol–gel process", *Chinese J. Aeronaut.*, https://doi.org/10.1016/j.cja.2020.07.004.

Huang, X., Zhang, Y., Moradi, Z. and Shafiei, N. (2021), "Computer simulation via a couple of homotopy perturbation methods and the generalized differential quadrature method for nonlinear vibration of functionally graded non-uniform micro-tube", *Eng. Comput.* https://doi.org/10.1007/s00366-021-01395-7.

Hussain, M., Naeem, M.N., Tounsi, A. and Taj, M. (2019), "Nonlocal effect on the vibration of armchair and zigzag SWCNTs with bending rigidity", *Adv. Nano Res., Int. J.*, **7**(6), 431-442. https://doi.org/10.12989/anr.2019.7.6.431.

Jam, J. and Kiani, Y. (2015), "Buckling of pressurized functionally graded carbon nanotube reinforced conical shells", *Compos. Struct.*, **125**, 586-595. https://doi.org/10.1016/j.compstruct.2015.02.052.

Jermsittiparsert, K., Ghabussi, A., Forooghi, A., Shavalipour, A., Habibi, M., won Jung, D. and Safa, M. (2020), "Critical voltage, thermal buckling and frequency characteristics of a thermally affected GPL reinforced composite microdisk covered with piezoelectric actuator", *Mech. Based Des. Struct.*, 1-23. https://doi.org/10.1080/15397734.2020.1748052.

Kar, K., Kumar, P., Iyengar, N. and Agnihotri, P. (1813), "Carbon nanotube and nanoparticles coated carbon fiber reinforced polymer hybrid composite with improved thermomechanical properties and a process for preparation thereof", Indian Patent.

Lei, Z., Liew, K. and Yu, J. (2013), "Buckling analysis of functionally graded carbon nanotube-reinforced composite plates using the element-free kp-Ritz method", *Compos. Struct.*, **98**, 160-168. https://doi.org/10.1016/j.compstruct.2012.11.006.

Li, H., Tang, J., Kang, Y., Zhao, H., Fang, D., Fang, X., Chen, R. and Wei, Z. (2018), "Optical properties of quasi-type-II structure in GaAs/GaAsSb/GaAs coaxial single quantum-well nanowires", *Appl. Phys. Lett.*, **113**(23), 233104. https://doi.org/10.1063/1.5053844.

Li, X., Feng, Y., Liu, B., Yi, D., Yang, X., Zhang, W., Chen, G., Liu, Y. and Bai, P. (2019), "Influence of NbC particles on microstructure and mechanical properties of AlCoCrFeNi high-entropy alloy coatings prepared by laser cladding", *J. Alloy. Compd.*, **788**, 485-494. https://doi.org/10.1016/j.jallcom.2019.02.223.

Li, Y., Jiang, J.-W., Zhu, W. and Chang, T. (2020), "Buckling of cylindrical shells subjected to a finite number of lateral loads: Application to single-walled carbon nanotubes", *Nanotechnology*, **31**(20), 205711. https://doi.org/10.1088/1361-6528/ab72b8.

Lim, C.W., Zhang, G. and Reddy, J.N. (2015), "A higher-order nonlocal elasticity and strain gradient theory and its applications in wave propagation", *J. Mech. Phys. Solids*, **78**, 298-313. https://droi.org/10.1016/j.jmps.2015.02.001.

Liu, M., Li, C., Cao, C., Wang, L., Li, X., Che, J., Yang, H., Zhang, X., Zhao, H., He, G. and Liu, X. (2021), "Walnut fruit processing equipment: Academic insights and perspectives", *Food Eng. Rev.*, https://doi.org/10.1007/s12393-020-09273-6.

Lu, H., Zhu, Y., Yuan, Y., He, L., Zheng, B., Zheng, X., Liu, C. and Du, H. (2021), "LiFSI as a functional additive of the fluorinated electrolyte for rechargeable Li-S batteries", *J. Mater. Sci.: Mater. El.*, **32**(5), 5898-5906. https://doi.org/10.1007/s10854-021-05310-0.

Luo, H., Shi, Z., Li, N., Gu, Z. and Zhuang, Q. (2001), "Investigation of the electrochemical and electrocatalytic behavior of single-wall carbon nanotube film on a glassy carbon electrode", *Anal. Chem.*, **73**(5), 915-920. https://doi.org/10.1021/ac000967l.

Ma, L.H., Ke, L.L., Reddy, J.N., Yang, J., Kitipornchai, S. and Wang, Y.S. (2018), "Wave propagation characteristics in magneto-electro-elastic nanoshells using nonlocal strain gradient theory", *Compos. Struct.*, **199**, 10-23. https://doi.org/10.1016/j.compstruct.2018.05.061.

Malikan, M. (2020), "On the plastic buckling of curved carbon nanotubes", *Theor. Appl. Mech. Lett.*, **10**(1), 46-56. https://doi.org/10.1016/j.taml.2020.01.004.

Malikan, M. and Eremeyev, V.A. (2020), "Post-critical buckling of truncated conical carbon nanotubes considering surface effects embedding in a nonlinear Winkler substrate using the Rayleigh-Ritz method", *Mater. Res. Express*, https://doi.org/10.1088/2053-1591/ab691c.

Malikan, M., Eremeyev, V.A. and Sedighi, H.M. (2020), "Buckling analysis of a non-concentric double-walled carbon nanotube", *Acta Mechanica*, **231**(12), 5007-5020. https://doi.org/10.1007/s00707-020-02784-7.

Matouk, H., Bousahla, A.A., Heireche, H., Bourada, F., Bedia, E., Tounsi, A., Mahmoud, S., Tounsi, A. and Benrahou, K. (2020), "Investigation on hygro-thermal vibration of P-FG and symmetric S-FG nanobeam using integral Timoshenko beam theory", *Adv. Nano Res., Int. J.*, **8**(4), 293-305. https://doi.org/10.12989/anr.2020.8.4.293.

Mehar, K. and Panda, S.K. (2019), "Multiscale modeling approach for thermal buckling analysis of nanocomposite curved structure", *Adv. Nano Res., Int. J.*, **7**(3), 181-190. http://doi.org/10.12989/anr.2019.7.3.181.

Mindlin, R.D. (1965), "Second gradient of strain and surface-tension in linear elasticity", *Int. J. Solids. Struct.*, **1**(4), 417-438. https://doi.org/10.1016/0020-7683(65)90006-5.

Mirjavadi, S.S., Matin, A., Shafiei, N., Rabby, S. and Mohasel Afshari, B. (2017a), "Thermal buckling behavior of two-dimensional imperfect functionally graded microscale-tapered porous beam", *J. Therm. Stresses*, **40**(10), 1201-1214. https://doi.org/10.1080/01495739.2017.1332962.

Mirjavadi, S.S., Mohasel Afshari, B., Shafiei, N., Rabby, S. and Kazemi, M. (2017b), "Effect of temperature and porosity on the vibration behavior of two-dimensional functionally graded micro-scale Timoshenko beam", *J. Vib. Control*, **24**(18), 4211-4225. https://doi.org/10.1177/1077546317721871.

Mirjavadi, S.S., Rabby, S., Shafiei, N., Afshari, B.M. and Kazemi, M. (2017c), "On size-dependent free vibration and thermal buckling of axially functionally graded nanobeams in thermal environment", *Appl. Phys. A.*, **123**(5), 315. https://doi.org/10.1007/s00339-017-0918-1.

Moayedi, H., Habibi, M., Safarpour, H., Safarpour, M. and Foong, L.K. (2019), "Buckling and Frequency Responses of a Graphene Nanoplatelet Reinforced Composite Microdisk", *Int. J. Appl. Mech.*, **11**(10), 1950102. https://doi.org/10.1142/S1758825119501023.

Mohamed, N., Mohamed, S.A. and Eltaher, M.A. (2020), "Buckling and post-buckling behaviors of higher order carbon nanotubes using energy-equivalent model", *Eng. Comput.* https://doi.org/10.1007/s00366-020-00976-2.

Moradi-Dastjerdi, R. and Malek-Mohammadi, H. (2017), "Biaxial buckling analysis of functionally graded nanocomposite sandwich plates reinforced by aggregated carbon nanotube using improved high-order theory", *J. Sandw. Struct. Mater.*, **19**(6), 736-769. https://doi.org/10.1177/1099636216643425.

Morasaei, A., Ghabussi, A., Aghlmand, S., Yazdani, M., Baharom, S. and Assilzadeh, H. (2021), "Simulation of steel–concrete

composite floor system behavior at elevated temperatures via multi-hybrid metaheuristic framework", *Eng. Comput.* https://doi.org/10.1007/s00366-020-01228-z.

Nejadi, M.M. and Mohammadimehr, M. (2020), "Buckling analysis of nano composite sandwich Euler-Bernoulli beam considering porosity distribution on elastic foundation using DQM", *Adv. Nano Res., Int. J.*, **8**(1), 59-68. https://doi.org/10.12989/anr.2020.8.1.059.

Noroozi, R., Barati, A., Kazemi, A., Norouzi, S. and Hadi, A. (2020), "Torsional vibration analysis of bi-directional FG nano-cone with arbitrary cross-section based on nonlocal strain gradient elasticity", *Adv. Nano Res., Int. J.*, **8**(1), 13-24. https://doi.org/10.12989/anr.2020.8.1.013.

Reddy, J.N. (2007), "Nonlocal theories for bending, buckling and vibration of beams", *Int. J. Eng. Sci.*, **45**(2), 288-307. https://doi.org/10.1016/j.ijengsci.2007.04.004.

Safarpour, M., Ghabussi, A., Ebrahimi, F., Habibi, M. and Safarpour, H. (2020), "Frequency characteristics of FG-GPLRC viscoelastic thick annular plate with the aid of GDQM", *Thin. Wall. Struct.*, **150**, 106683. https://doi.org/10.1016/j.tws.2020.106683.

Semmah, A., Heireche, H., Bousahla, A.A. and Tounsi, A. (2019), "Thermal buckling analysis of SWBNNT on Winkler foundation by non local FSDT", *Adv. Nano Res., Int. J.*, **7**(2), 89-98. http://doi.org/10.12989/anr.2019.7.2.089.

Shafiei, N. and Kazemi, M. (2017), "Buckling analysis on the bi-dimensional functionally graded porous tapered nano-/micro-scale beams", *Aerosp. Sci. Technol.*, **66**, 1-11. https://doi.org/10.1016/j.ast.2017.02.019.

Shafiei, N. and She, G.-L. (2018), "On vibration of functionally graded nano-tubes in the thermal environment", *Int. J. Eng. Sci.*, **133**, 84-98. https://doi.org/10.1016/j.ijengsci.2018.08.004.

Shafiei, N., Kazemi, M. and Ghadiri, M. (2016a), "On size-dependent vibration of rotary axially functionally graded microbeam", *Int. J. Eng. Sci.*, **101**, 29-44. https://doi.org/10.1016/j.ijengsci.2015.12.008.

Shafiei, N., Mousavi, A. and Ghadiri, M. (2016b), "Vibration behavior of a rotating non-uniform FG microbeam based on the modified couple stress theory and GDQEM", *Compos. Struct.*, **149**, 157-169. https://doi.org/10.1016/j.compstruct.2016.04.024.

Shafiei, N., Ghadiri, M., Makvandi, H. and Hosseini, S.A. (2017a), "Vibration analysis of Nano-Rotor's Blade applying Eringen nonlocal elasticity and generalized differential quadrature method", *Appl. Math. Model.*, **43**, 191-206. https://doi.org/10.1016/j.apm.2016.10.061.

Shafiei, N., Kazemi, M. and Fatahi, L. (2017b), "Transverse vibration of rotary tapered microbeam based on modified couple stress theory and generalized differential quadrature element method", *Mech. Adv. Mater. Struct.*, **24**(3), 240-252. https://doi.org/10.1080/15376494.2015.1128025.

Shafiei, N., Ghadiri, M. and Mahinzare, M. (2019), "Flapwise bending vibration analysis of rotary tapered functionally graded nanobeam in thermal environment", *Mech. Adv. Mater. Struct.*, **26**(2), 139-155. 10.1080/15376494.2017.1365982.

Shams, S. and Soltani, B. (2017), "The effects of carbon nanotube waviness and aspect ratio on the buckling behavior of functionally graded nanocomposite plates using a meshfree method", *Polym. Compos.*, **38**, E531-E541. https://doi.org/10.1002/pc.23814.

Shariati, A., Ghabussi, A., Habibi, M., Safarpour, H., Safarpour, M., Tounsi, A. and Safa, M. (2020a), "Extremely large oscillation and nonlinear frequency of a multi-scale hybrid disk resting on nonlinear elastic foundation", *Thin-Wall. Struct.*, **154**, 106840. https://doi.org/10.1016/j.tws.2020.106840.

Shariati, A., Jung, D.W., Mohammad-Sedighi, H., Żur, K.K., Habibi, M. and Safa, M. (2020b), "Stability and dynamics of viscoelastic moving rayleigh beams with an asymmetrical distribution of material parameters", *Symmetry*, **12**(4), 586. https://doi.org/10.3390/sym12040586.

Shivanian, E., Ghadiri, M. and Shafiei, N. (2017), "Influence of size effect on flapwise vibration behavior of rotary microbeam and its analysis through spectral meshless radial point interpolation", *Appl. Phys. A.*, **123**(5), 329. https://doi.org/10.1007/s00339-017-0955-9.

Sui, M., Li, C., Wu, W., Yang, M., Ali, H.M., Zhang, Y., Jia, D., Hou, Y., Li, R. and Cao, H. (2021), "Temperature of grinding carbide with castor oil-based MoS_2 nanofluid minimum quantity lubrication", *J. Therm. Sci. Eng. Applicat.*, **13**(5), 051001. https://doi.org/10.1115/1.4049982.

Tounsi, A., Benguediab, S., Semmah, A. and Zidour, M. (2013), "Nonlocal effects on thermal buckling properties of double-walled carbon nanotubes", *Adv. Nano Res., Int. J.*, **1**(1), 1-11. http://doi.org/10.12989/anr.2013.1.1.001.

Uzun, B. and Civalek, Ö. (2019), "Free vibration analysis Silicon nanowires surrounded by elastic matrix by nonlocal finite element method", *Adv. Nano Res., Int. J.*, **7**(2), 99-108. http://doi.org/10.12989/anr.2019.7.2.099.

Wallace, J., Chen, D. and Shao, L. (2020), "Irradiation-enhanced torsional buckling capacity of carbon nanotube bundles", *J. Appl. Phys.*, **128**(19), 195902. https://doi.org/10.1063/5.0013229.

Wang, Y., Li, C., Zhang, Y., Yang, M., Li, B., Jia, D., Hou, Y. and Mao, C. (2016), "Experimental evaluation of the lubrication properties of the wheel/workpiece interface in minimum quantity lubrication (MQL) grinding using different types of vegetable oils", *J. Clean. Prod.*, **127**, 487-499. https://doi.org/10.1016/j.jclepro.2016.03.121.

Wang, X., Li, C., Zhang, Y., Ding, W., Yang, M., Gao, T., Cao, H., Xu, X., Wang, D., Said, Z., Debnath, S., Jamil, M. and Ali, H.M. (2020), "Vegetable oil-based nanofluid minimum quantity lubrication turning: Academic review and perspectives", *J. Manuf. Process.*, **59**, 76-97. https://doi.org/10.1016/j.jmapro.2020.09.044.

Wang, J.F., Cao, S.H. and Zhang, W. (2021a), "Thermal vibration and buckling analysis of functionally graded carbon nanotube reinforced composite quadrilateral plate", *Eur. J. Mech.-A*, **85**, 104105. https://doi.org/10.1016/j.euromechsol.2020.104105.

Wang, P., Li, Z., Xie, Q., Duan, W., Zhang, X. and Han, H. (2021b), "A passive anti-icing strategy based on a superhydrophobic mesh with extremely low ice adhesion strength", *J. Bionic Eng.*, **18**(1), 55-64. https://doi.org/10.1007/s42235-021-0012-4.

Wu, H., Kitipornchai, S. and Yang, J. (2015), "Free vibration and buckling analysis of sandwich beams with functionally graded carbon nanotube-reinforced composite face sheets", *Int. J. Struct. Stab. Dyn.*, **15**(7), 1540011. https://doi.org/10.1142/S0219455415400118.

Wu, C.-P., Chen, Y.-H., Hong, Z.-L. and Lin, C.-H. (2018), "Nonlinear vibration analysis of an embedded multi-walled carbon nanotube", *Adv. Nano Res., Int. J.*, **6**(2), 163-182. http://doi.org/10.12989/anr.2018.6.2.163.

Yang, J. and Shen, H.-S. (2002), "Vibration characteristics and transient response of shear-deformable functionally graded plates in thermal environments", *J. Sound Vib.*, **255**(3), 579-602. https://doi.org/10.1006/jsvi.2001.4161.

Yin, Q., Li, C., Dong, L., Bai, X., Zhang, Y., Yang, M., Jia, D., Li, R. and Liu, Z. (2021), "Effects of physicochemical properties of different base oils on friction coefficient and surface roughness in MQL milling AISI 1045", *Int. J. Precis. Eng. Manuf.-Green Technol.*, https://doi.org/10.1007/s40684-021-00318-7.

Zeighampour, H. and Tadi, B.Y. (2020), "Buckling analysis of boron nitride nanotube with and without defect using molecular dynamic simulation", *Mol. Simulat.*, **46**(4), 279-288. https://doi.org/10.1080/08927022.2019.1697817.

Zghal, S., Trabelsi, S. and Dammak, F. (2020), "Post-buckling behavior of functionally graded and carbon-nanotubes based structures with different mechanical loadings", *Mech. Based Des. Struct.*, 1-43. https://doi.org/10.1080/15397734.2020.1790387.

Zhang, Y., Li, C., Jia, D., Zhang, D. and Zhang, X. (2015), "Experimental evaluation of the lubrication performance of MoS_2/CNT nanofluid for minimal quantity lubrication in Ni-based alloy grinding", *Int. J. Mach. Tool. Manuf.*, **99**, 19-33. https://doi.org/10.1016/j.ijmachtools.2015.09.003.

Zhang, Y., Li, C., Ji, H., Yang, X., Yang, M., Jia, D., Zhang, X., Li, R. and Wang, J. (2017), "Analysis of grinding mechanics and improved predictive force model based on material-removal and plastic-stacking mechanisms", *Int. J. Mach. Tool. Manuf.*, **122**, 81-97. https://doi.org/10.1016/j.ijmachtools.2017.06.002.

Zhang, K., Huo, Q., Zhou, Y.-Y., Wang, H.-H., Li, G.-P., Wang, Y.-W. and Wang, Y.-Y. (2019), "Textiles/metal–organic frameworks composites as flexible air filters for efficient particulate matter removal", *ACS Appl. Mater. Interf.*, **11**(19), 17368-17374. https://doi.org/10.1021/acsami.9b01734.

Zhang, J., Wu, W., Li, C., Yang, M., Zhang, Y., Jia, D., Hou, Y., Li, R., Cao, H. and Ali, H.M. (2020a), "Convective heat transfer coefficient model under nanofluid minimum quantity lubrication coupled with cryogenic air grinding Ti–6Al–$_4$V", *Int. J. Precis. Eng. Manuf.-Green Technol.*, 1-23. https://doi.org/10.1007/s40684-020-00268-6.

Zhang, K., Yang, Z., Mao, X., Chen, X.-L., Li, H.-H. and Wang, Y.-Y. (2020b), "Multifunctional textiles/metal−organic frameworks composites for efficient ultraviolet radiation blocking and noise reduction", *ACS Appl. Mater. Interf.*, **12**(49), 55316-55323. https://doi.org/10.1021/acsami.0c18147.

JL